

RESEARCH ARTICLE

Targeted modulation of gene expression through receptor-specific delivery of small interfering RNA peptide conjugates

Mareike Schenk¹ | Karin Mörl¹ | Stephan Herzig^{2,3} | Annette G. Beck-Sickinger¹ 

¹Institute of Biochemistry, Faculty of Life Sciences, Leipzig University, Leipzig, Germany

²Institute for Diabetes and Cancer, Helmholtz Munich, German Center for Diabetes Research (DZD), Neuherberg, Germany

³Department of Endocrinology, Diabetology, Metabolism and Clinical Chemistry (Internal Medicine 1), Heidelberg University Hospital, Heidelberg, Germany

Correspondence

Annette G. Beck-Sickinger, Institute of Biochemistry, Faculty of Life Sciences, Leipzig University, Brüderstrasse 34, 04103 Leipzig, Germany.

Email: abeck-sickinger@uni-leipzig.de

Funding information

HI-MAG; Deutsche Forschungsgemeinschaft, Grant/Award Number: SFB 1052-B04, project number 209933838

Small interfering RNA (siRNA) has emerged as a valuable tool to address RNA interference (RNAi) to modulate gene expression also in therapy. However, challenges such as inefficient cell targeting and rapid degradation in biological systems have limited its success. To address these issues, the development of a receptor-specific shuttle system represents a promising solution. [⁷F, ³⁴P]-NPY analogues were modified by solid-phase peptide synthesis, enabling non-covalent conjugation with siRNA. This modification yielded an efficient siRNA vehicle capable of binding and transporting its cargo into target cells without adversely affecting receptor activation or cell viability. Mass spectrometry and gel shift assays confirmed successful and stable siRNA binding under various conditions. Microscopy experiments further demonstrated the co-internalization of labeled peptides and siRNA in Hepa1c1 cells, highlighting the stability of the complex. In vitro quantitative RT-PCR experiments, targeting the TSC22D4 gene to normalize systemic glucose homeostasis and insulin resistance, revealed a functional peptide-based siRNA shuttle system with the ability to decrease mRNA expression to approximately 40%. These findings strengthen the potential of receptor-specific siRNA shuttle systems as efficient tools for gene therapy that offer a possibility for reducing side effects.

KEYWORDS

biological activity, drug delivery, gene expression, oligonucleotides, peptides, receptors, siRNA

1 | INTRODUCTION

Findings in the late 1990s and early 2000s on RNA interference (RNAi) and small interfering RNA (siRNA) laid the groundwork to explore the possibilities of making previously considered undruggable targets accessible.^{1–4} The RNA-induced silencing complex (RISC)

recognizes siRNA as a double strand, selectively discarding one strand before binding to the target mRNA. This precise mechanism results in gene silencing with remarkable efficiency that requires only a few double-stranded RNA molecules per cell.^{1,5} While siRNAs hold immense potential for medical applications, the practical application is still challenging. Despite their advantages, such as low production

Abbreviations: Adm, adamantylpropionyl; arr-3, arrestin-3; BRET, bioluminescence resonance energy transfer; CF, carboxyfluorescein; Dde, 1-(4,4-dimethyl-2,6-dioxocyclohex-1-ylidene)ethyl; DIC, *N,N*-diisopropylcarbodiimide; DIPEA, *N,N*-diisopropylethylamine; DMEM, Dulbecco's modified Eagle's medium; DMF, *N,N*-dimethylformamide; DODT, 3,6-dioxo-1,8-octanedithiol; ESI, electron spray ionization; FBS, fetal bovine serum; FDA, Food and Drug Administration; Fmoc, 9-fluorenylmethoxycarbonyl; HATU, 1-[bis(dimethylamino)methylene]-1*H*-1,2,3-triazolo[4,5-*b*]pyridinium 3-oxide hexafluorophosphate; HBSS, Hank's balanced salt solution; HEPES, 4-(2-hydroxyethyl)-1-piperazineethanesulfonic acid; HTRF, homogeneous time-resolved fluorescence; IP1, inositol monophosphate; Lau, lauroyl; Mmt, monomethoxytrityl; NEAA, non-essential amino acids; Nluc, nanoluciferase; NPY, neuropeptide Y; Oxyma, ethylcyanohydroxyiminoacetate; PAA, polyacrylamide; RISC, RNA-induced silencing complex; RNAi, RNA interference; siRNA, small interfering RNA; SPPS, solid-phase peptide synthesis; TA, thioanisole; TAMRA, TAM, 6-carboxytetramethylrhodamine; tBu, *tert*-butyl; TFA, trifluoroacetic acid; TIS, triisopropylsilane; TSC22D4, growth factor- β 1 stimulated clone 22 D4; Y₁R, Y₁ receptor.

This is an open access article under the terms of the [Creative Commons Attribution-NonCommercial](https://creativecommons.org/licenses/by-nc/4.0/) License, which permits use, distribution and reproduction in any medium, provided the original work is properly cited and is not used for commercial purposes.

© 2024 The Authors. *Journal of Peptide Science* published by European Peptide Society and John Wiley & Sons Ltd.

costs and ease of synthesis, issues to be resolved include degradation and delivery without inducing toxicity or other adverse effects.⁶⁻⁸ Despite these challenges, Alnylam Pharmaceuticals defied expectations by securing approval from the US Food and Drug Administration (FDA) for Onpattro (patisiran) in 2018, marking the first FDA-approved RNA interference (RNAi) drug.⁹ However, ongoing research aims to address remaining shortcomings and enhance siRNA drug delivery methods.¹⁰⁻¹³

In targeted therapy, an effective delivery tool must fulfill multiple criteria, including delivery to and accumulation in the target tissue, preventing nuclease degradation as well as immune-related toxicity.⁸ Once the siRNA reaches the target tissue, it successfully has to manage endosomal and lysosomal escape to recruit proteins and enzymes integral to the RISC. Various delivery platforms, such as lipids, polymers, conjugates, nanoparticles, and peptides, have been explored so far, facing challenges related to toxicity and selective delivery, particularly delivery to extrahepatic tissues.¹⁴⁻²⁴

Peptides, serving as ligands in ligand-receptor interaction, present an interesting option because of their biocompatibility, biodegradability, and ease of modification.^{25,26}

Utilizing peptide ligands as a delivery platform offers the advantage of selective binding to cells expressing the corresponding receptor. By attaching a linker to the peptide carrier, covalent or non-covalent binding of the siRNA drug molecule is enabled, facilitating delivery to the receptor and entry into the cell. A schematic representation of this approach is shown in Figure 1.

The neuropeptide Y₁ system emerges as a promising target due to its high selectivity and affinity. Its native ligand NPY was further optimized to the selective analogue [F⁷,P³⁴]-NPY and to short variants [K²⁷(Adm),P³⁰,K³¹,Bip³²,L³⁴]-NPY(27-36) and [K²⁷(Lau),P³⁰,K³¹,Bip³²,L³⁴]-NPY(27-36).^{27,28} These analogues exhibit enhanced selectivity for the Y₁ receptor (Y₁R) and nanomolar potency, making them powerful candidates as shuttle systems. These three different peptides were modified with a lysine linker to enable siRNA binding. Either

L- or D-lysine was investigated in the linker with respect to their application as siRNA shuttling system for targeted delivery.

The tested siRNA sequence targets the growth factor- β 1 stimulated clone 22 D4 (TSC22D4) gene, which interacts with protein kinase B/Akt1 thus being a part of the insulin/phosphatidylinositol 3-kinase signaling pathway.²⁹ It was shown that TSC22D4 regulates insulin signaling and glucose metabolism and plays a role in tumor formation and so provides an interesting target for therapeutic approaches.²⁹⁻³¹

2 | METHODS

2.1 | General methods

For automated peptide synthesis, a Multisynth/Biotage Syro I synthesis robot was used. Peptide purity was determined by analytical reversed-phase HPLC using a Phenomenex Jupiter[®] 4 U Proteo C12 90 Å (250 × 4.6 mm, 4 μm, 90 Å) and a Phenomenex AeriS[®] Peptide 3.6 U XBC18 (250 × 4.6 mm, 3.6 μm, 100 Å) column. Mass spectra were measured by electron spray ionization (ESI) using a Thermo Scientific Orbitrap Elite mass spectrometer. Live cell imaging was performed with a Molecular Devices High-Content Imaging System and a Zeiss Axio Observer.Z1 microscope with an additional ApoTome.2 imaging system. Receptor activation assays, cell viability assays, and NanoBRET arrestin-3 recruitment assays were performed using a Tecan Spark Plate Reader.

2.2 | Peptide synthesis

Peptides were synthesized in a combination of manual coupling and automated solid phase peptide synthesis (SPPS) on a SYRO I synthesis robot (Multisynth/Biotage) by 9-fluorenylmethoxycarbonyl

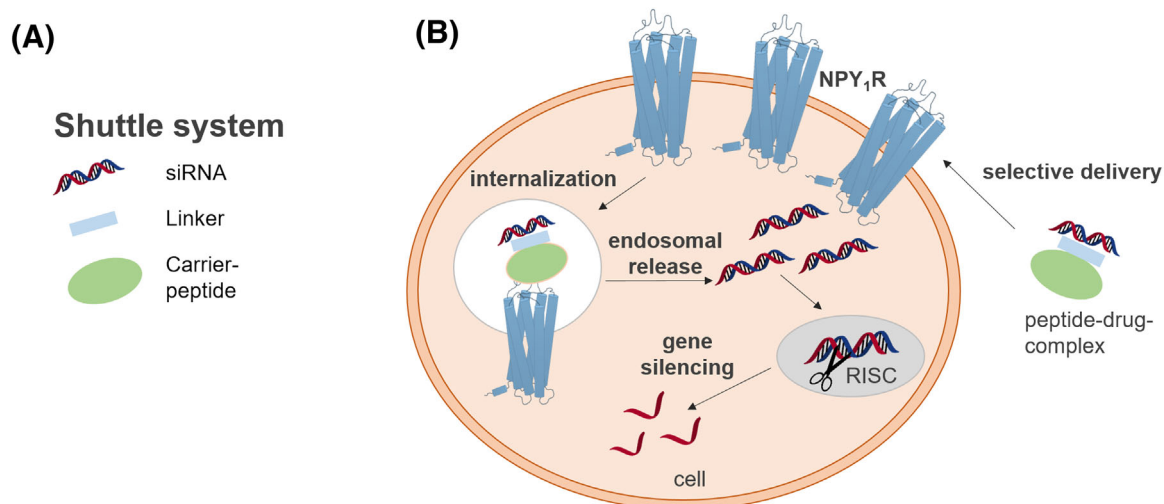


FIGURE 1 Schematic representation of the setup of the shuttle system (A) and cellular processes from delivery to internalization, endosomal release of siRNA, binding to RISC and mRNA degradation (B).

(Fmoc)/*tert*-butyl (tBu) protection group strategy on a TentaGel resin Rink amide (TGR RAM, IRIS Biotech GmbH) resin with a loading capacity of 0.1–0.2 mmol g⁻¹ and a scale of 15 μmol per peptide. During automated synthesis, double coupling procedures were performed with 8 eq. of amino acid, ethyl cyanohydroxyiminoacetate (Oxyma) and *N,N*-diisopropylcarbodiimide (DIC) and a reaction time of 42 min per cycle. Fmoc cleavage was performed in two subsequent cycles by applying 40% and 20% piperidine in *N,N*-dimethylformamide (DMF) for 3 and 10 min, respectively. Lysine side chains were protected either with a 1-(4,4-dimethyl-2,6-dioxocyclohex-1-ylidene)ethyl (Dde) or monomethoxytrityl (Mmt) protecting group. For Dde cleavage, the resin was treated in 10 subsequent cycles with 2% hydrazine in DMF for 10 min each. Mmt cleavage was performed in 15 subsequent cycles using a cleavage solution of 2% trifluoroacetic acid (TFA) and 5% triisopropylsilane (TIS) in DCM. Labeling was achieved with 6-carboxytetramethylrhodamine (TAMRA) fluorophore by incubation of the fluorophore (0.015 mmol, 2 eq.) and 1-[bis(dimethylamino)methylene]1*H*-1,2,3-triazolo[4,5-*b*]pyridinium-3-oxidehexa-fluorophosphate (HATU, 0.014 mmol, 1.9 eq.) dissolved in 400 μl DMF and 2.6 μl (0.015 mmol, 2 eq.) *N,N*-diisopropylethylamine (DIPEA) for 16 h shaking at 25°C. After incubation, surplus material was washed off using DCM. The peptides were cleaved from the resin, and remaining protection groups were removed by incubation with 90% TFA and 10% thioanisole (TA)/3,6-dioxa-1,8octanedithiol (DODT) mixture (7:3, v/v) for 3 h by shaking at 25°C and precipitated from ice-cold diethyl ether. The remaining scavenger was removed by several washing steps with ice-cold diethyl ether. Solvent was removed by lyophilization.

For purification, the crude peptide was dissolved in acetonitrile/H₂O, and the fluorophore labeled peptide was separated from side products by using reversed-phase HPLC (RP-HPLC). Resulting fractions were analyzed by mass spectrometry and analytical RP-HPLC; fractions containing more than 95% pure product were combined. Prior to lyophilization, the resulting product was again analyzed by mass spectrometry and two different RP-HPLC systems to confirm identity and purity.

2.3 | Preparation of siRNA and peptide–siRNA complex

To duplex sense and antisense strand of siRNA (Biomers) equal amounts were incubated for 1 min at 90°C, slowly cooled down to 37°C, and then incubated for 1 h at 37°C. For complexation of siRNA duplex and peptide, both compounds were incubated in a ratio of either 1:1 or 1:5 (siRNA/peptide) for 15 min at 37°C. For confirmation of duplexation and complexation, gel shift assay with a native polyacrylamide (PAA) was performed. A 12.5% PAA solution was supplemented with APS and TEMED for polymerization prior to casting the gel. Native RNA loading dye was added to samples, and run was performed at 120 V for 90 min. Detection was performed by fluorescence as siRNA was labeled with carboxyfluorescein.

2.4 | Cell culture

All cell lines were cultured at 37°C and 5% CO₂ in a humidified atmosphere. Stably transfected human embryo kidney cells HEK293 hY₁R_eYFP were cultured in Dulbecco's modified Eagle's medium (DMEM) mixed with Ham's F12 (1:1, Lonza) and supplemented with 15% (v/v) heat-inactivated fetal bovine serum (FBS) and 100 μg mL⁻¹ hygromycin B (Invitrogen). Stably transfected African green monkey cells COS-7 hY_{1/2/4/5}R_eYFP were cultured in DMEM supplemented with 10% (v/v) FBS, 1.5 mg mL⁻¹ G418 and 133 μg mL⁻¹ hygromycin B (Invitrogen). For murine hepatoma cells (Hepa1c1c7) DMEM is supplemented with 10% (v/v) FBS, 1% non-essential amino acids (NEAA), and 1% penicillin–streptomycin (Gibco).

2.5 | Cell viability assay

To test the influence of either peptide, siRNA, or peptide–siRNA complex on cell viability when administered to living cells, a resazurin-based cell viability assay was utilized. Hepa1c1c7 cells (10,000 cells/well) were seeded in a sterile 96-well plate and cultured overnight under standard incubation conditions. Compounds were diluted to a final concentration of 50 μM for peptides, 50 μM peptide and 10 μM siRNA for peptide–siRNA complex, and 10 μM for siRNA. Cell culture medium was aspirated from cells and replaced with compound containing medium or cell culture media only serving as negative control. After 24 h of incubation at 37°C, cells were washed twice with serum-free cell culture medium and then incubated for 2 h with 10% (v/v) resazurin (Sigma-Aldrich) in serum-free cell culture medium under standard incubation conditions. In addition, cells were incubated for 10 min with 70% (v/v) ethanol in water before adding resazurin solution for positive control. As living cells reduce non-fluorescent resazurin to resorufin, cell viability can be quantified by fluorescence measurement ($\lambda_{ex} = 550$ nm, $\lambda_{em} = 595$ nm) using a plate reader (Tecan Spark, Tecan). Measurements were normalized to negative control (100% cell viability). All peptide concentrations were tested in technical triplicates, and experiments were performed in three biological replicates.

2.6 | Receptor activation assay

The influence of peptide modification and siRNA complexation on the ligands' ability to activate the human Y₁R receptor selectively was investigated by an inositol monophosphate accumulation assay (IP-One assay, Cisbio). Stably transfected COS-7_hY₁R_ΔGq cells were seeded (6000 cells/well) into white 384-well microplates (Greiner Bio-One) and grown for 24 h under standard culturing conditions. Compounds were solved in HBSS containing 20 mM LiCl (stimulation buffer) varying in peptide concentrations from 10⁻⁵ to 10⁻¹² M resulting from a serial dilution. Medium was removed prior to stimulation at 37°C and 5% CO₂ in humidified atmosphere for 45–60 min. After stimulation, 3 μl of cryptate-labeled antibody (FRET donor) and

IP1 coupled to d2 (FRET acceptor) diluted in lysis and detection buffer (1:20) as described in the manufacturer's protocol were added subsequently to the cells followed by 60 min incubation on a tumbler at room temperature. Homogeneous time-resolved fluorescence (HTRF) was measured at $\lambda_{ex} = 320$ nm and $\lambda_{em} = 620$ nm for the FRET donor and $\lambda_{ex} = 320$ nm and $\lambda_{em} = 665$ nm for the FRET acceptor using a plate reader (Tecan Spark, Tecan). Acceptor to donor ratio was calculated and plotted against peptide concentration. Data were analyzed using GraphPad Prism 10 (GraphPad Software, San Diego, USA), fitting dose response with standard slope and normalized to wild-type ligand response. EC₅₀ values are given as mean \pm SEM.

2.7 | NanoBRET Arrestin-3 recruitment assay

Arrestin recruitment was investigated with a NanoBRET-based assay as described previously.³² Arrestin-3 (arr-3) and a small nanoluciferase (Nluc)³³ are genetically fused serving as donor for bioluminescence resonance energy transfer (BRET), and the eYFP-labeled receptor acts as acceptor.

HEK293 cells were grown to 70%–80% confluency and transfected overnight with 100 ng of plasmid encoding arr-3 fused to the Nluc and 9900 ng of plasmid encoding the Y₁R C terminally fused to eYFP using Metafectene Pro (Biontex Laboratories GmbH) according to the manufacturer's protocol. On day one after transfection, cells were seeded (75,000 cells mL⁻¹) into poly-D-lysine coated solid white 96-well plates and incubated overnight at 37°C. On day 2 post-transfection, unlabeled peptides were serially diluted in BRET buffer (Hanks' balanced salt solution, 25 mM 4-(2-hydroxyethyl)-1-piperazineethanesulfonic acid (HEPES; Merck), pH 7.3) to concentrations ranging from 10⁻¹⁰ to 10⁻⁵ M. Cell medium was replaced by BRET buffer and coelenterazine H prior to stimulation with peptide ligand. The BRET signal was measured at 25°C after different time points (10 and 15 min) with a Tecan Spark plate reader (Tecan) observing luminescence signal from 400 to 440 nm for coelenterazine H and eYFP fluorescence signal from 505 to 590 nm. BRET signal was calculated as the ratio of the emission signals from fluorescence to luminescence. The netBRET was determined through baseline correction using the mean value calculated from control samples in unstimulated cells.

The assay was performed in quadruplicates in at least three independent experiments.

2.8 | Live cell microscopy

Internalization of peptide ligand and peptide–siRNA complex was investigated by live cell imaging. Hepa1c1c7 cells were seeded into sterile μ -slide 8 wells (Ibidi) and grown under standard cell culture conditions described above to a confluency of about 70%–80%. To ensure sufficient amount of receptor being present at the membrane, cells were starved in minimal medium (Opti-MEM™, Gibco) supplemented with Hoechst 33342 nuclear stain (Sigma-Aldrich) for 30–60 min at 37°C. Cells were treated with either peptide, siRNA, or peptide–siRNA

complex in varying concentrations for 30–120 min. After stimulation, several washing steps using acidic wash buffer (50 mM glycine, 100 mM NaCl in H₂O, pH 3.0) and Hank's balanced salt solution (HBSS) were performed. Microscopy images were taken in a quasi-confocal setting using an AxioObserver.Z1 microscope with an additional ApoTome.2 imaging system (Zeiss). All images were recorded using a fixed exposure time for each of the fluorescence channels. Experiments were performed in at least three independent experiments.

2.9 | siRNA delivery assay

Cells were seeded in either 6-, 12-, 24-, or 48-well plate and grown overnight to a confluency of 70%–80%. On the following day, media were replaced by fresh medium containing the corresponding peptide–siRNA complex. Cells were incubated for 6 h and further cultivated for 72 h after a media exchange. For experiments with Y₁ antagonist BIBP3226, cells were preincubated for 1 h with 1 mM of BIBP3226 prior administering peptide–siRNA complex.

2.10 | RNA isolation

For RNA isolation, RNeasy Mini Kit (Qiagen) was used according to the manufacturer's protocol. In brief, treated cells underwent lysis with a β -mercaptoethanol containing buffer and ethanol, followed by several washing steps and an additional DNase I digestion. Extracted RNA was eluted in RNase-free water, and concentration was determined in duplicates using a plate reader (Tecan Infinite 200, Tecan). Samples were either directly further processed or stored at –70°C.

2.11 | Quantitative real-time PCR

Changes of gene expression on mRNA level were investigated with quantitative PCR (qPCR) experiments using GoTaq® Probe 1-Step RT-qPCR System (Promega) and predesigned primers (QuantiTect® Primer Assays, Qiagen). Reaction mix was prepared according to the manufacturer's protocol. For control reactions, nuclease-free water was used as template. All samples were run in technical duplicates. Calculation of relative expression ratios was performed according to the $\Delta\Delta$ Ct method using expression of a reference gene as well as samples from cells untreated or treated with only peptide. Data represent the mean \pm SEM from at least three independent experiments performed in duplicates.

3 | RESULTS

3.1 | Peptide synthesis

The NPY receptor Y₁ is a well-known target for antiobesity drugs. It has been shown to be specifically addressed by a modified neuropeptide Y (NPY) analogue named [F⁷,P³⁴]NPY.^{27,34} By combining [F⁷,P³⁴]-

NPY and a distinct siRNA sequence, this molecule can be selectively transported to target cells expressing the NPY receptor Y₁. A peptide linker consisting of eight lysine residues has been introduced to bind the siRNA non-covalently to the peptide. To examine different NPY analogues regarding their suitability, three different peptide backbones were synthesized, each equipped with either an L-lysine or a D-lysine linker. For the full-length NPY derivatives, the octalysine linker is attached to the lysine at position 4 of the backbone. In the short NPY variants, the lysine at position 31 is used for the introduction of the linker. Additionally, the peptides were synthesized with or without fluorophore labels resulting in 12 different peptides. In the case of fluorophore labeling, the fluorophore is attached at the end of the lysine linker. The peptides were purified by preparative RP-HPLC to a purity >95%. This was confirmed via MALDI-ToF-MS and analytical RP-HPLC. Detailed analytical data and sequence of each peptide are shown in Table 1.

3.2 | Peptide–siRNA complex

The siRNA sequence is directed against TSC22D4, which plays a crucial role in regulating insulin signaling and manages glucose levels at

the molecular level.³⁰ For analysis, the siRNA sequence was labeled with carboxyfluorescein (CF) to follow uptake and intracellular release. The siRNA sequence is provided in Table 2.

The formation of the complex of [F⁷,P³⁴]-NPY modified with a peptide linker consisting of either eight L- or D-lysines and siRNA was investigated. Data in Figure 2 show that the complex of peptide and siRNA is stable under the conditions used in gel shift assays (Figure 2A) and MALDI-ToF (Figure 2C). For complexes with short NPY analogues (3–6), native polyacrylamide gel shift assay (Figure 2B) was used to investigate complex formation. As expected and shown before,^{35–38} fully complexed siRNA does not migrate in the polyacrylamide gel but instead accumulated within the loading wells, and only a small amount of uncomplexed siRNA migrated through the gel.

TABLE 2 Sequence of siRNA targeting TSC22D4.

Strand	Sequence
Sense	5'-CF-GGACGUGUGUGGAUGUUUAdTdT-3'
Antisense	5'-UAAACAUCCACACAGUCCdTdT-3'

TABLE 1 Analytical data of synthesized peptides. MALDI-ToF or ESI ion trap MS confirmed peptide identity. Two different HPLC systems were used to quantify peptide purity. Elution of the peptide was determined from linear gradients of eluent B in eluent A (A: 0.1 % trifluoroacetic acid (TFA) in H₂O, B: 0.08 % TFA in acetonitrile (ACN)) on a Phenomenex Aeris Peptide C18 column (100 Å).

Peptide	Sequence	Purity [%]	Mass spectrometry		Elution [% ACN]
			M _{calc}	M _{found}	
1a	[K ⁴ (L-K ₈),F ⁷ ,P ³⁴]-NPY	>95	5278.89	5278.90	37.3
1b	[K ⁴ (L-K ₈ -TAM),F ⁷ ,P ³⁴]-NPY	>95	5690.05	5691.10	37.8
2a	[K ⁴ (D-K ₈),F ⁷ ,P ³⁴]-NPY	>95	5277.90	5278.92	36.6
2b	[K ⁴ (D-K ₈ -TAM),F ⁷ ,P ³⁴]-NPY	>95	5690.05	5691.05	37.3
3a	[K ²⁷ (Adm),P ³⁰ ,K ³¹ (L-K ₈),Bip ³² ,L ³⁴]-NPY(27-36)	>95	2623.74	2624.69	33.1
3b	[K ²⁷ (Adm),P ³⁰ ,K ³¹ (L-K ₈ -TAM),Bip ³² ,L ³⁴]-NPY(27-36)	>95	3035.88	3036.94	34.2
4a	[K ²⁷ (Adm),P ³⁰ ,K ³¹ (D-K ₈),Bip ³² ,L ³⁴]-NPY(27-36)	>95	2623.74	2624.51	33.0
4b	[K ²⁷ (Adm),P ³⁰ ,K ³¹ (D-K ₈ -TAM),Bip ³² ,L ³⁴]-NPY(27-36)	>95	3035.88	3036.89	34.3
5a	[K ²⁷ (Lau),P ³⁰ ,K ³¹ (L-K ₈),Bip ³² ,L ³⁴]-NPY(27-36)	>95	2615.77	2616.71	36.7
5b	[K ²⁷ (Lau),P ³⁰ ,K ³¹ (L-K ₈ -TAM),Bip ³² ,L ³⁴]-NPY(27-36)	>95	3027.91	3029.10	37.4
6a	[K ²⁷ (Lau),P ³⁰ ,K ³¹ (D-K ₈),Bip ³² ,L ³⁴]-NPY(27-36)	>95	2615.77	2616.57	36.7
6b	[K ²⁷ (Lau),P ³⁰ ,K ³¹ (D-K ₈ -TAM),Bip ³² ,L ³⁴]-NPY(27-36)	>95	3027.91	3028.89	37.5
7	[F ⁷ ,P ³⁴]-NPY	>95	4253.14	4254.23	38.9

Abbreviations: Adm, adamantyl; Bip, biphenylalanine; Lau, lauryl; TAM, 6-carboxytetramethylrhodamine.

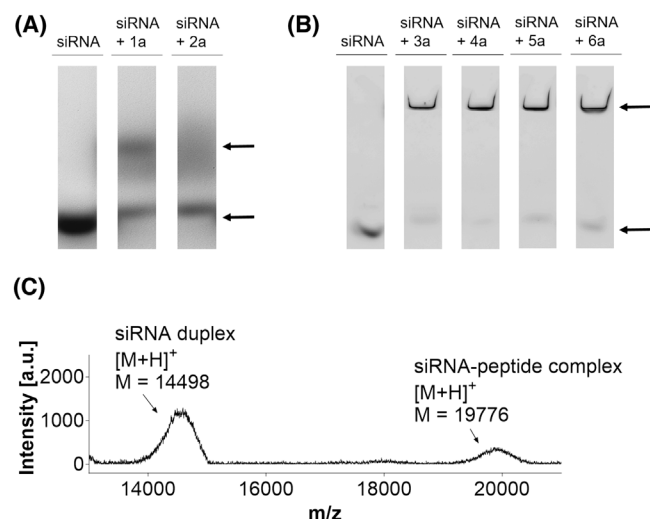


FIGURE 2 Characterization of $[F^7,P^{34}]$ -NPY and siRNA complexation in a ratio of 1:1. (A) Agarose gel with siRNA only and siRNA complexed with either **1a** or **2a** is shown by the resulting upward shift. (B) Native polyacrylamide gel with siRNA only and siRNA complexed with either **3a**, **4a**, **5a**, or **6a** is shown. (C) MALDI-ToF analysis of $[K^4(K_8),F^7,P^{34}]$ -NPY-siRNA (**1a**) complex displaying siRNA duplex and $[K^4(K_8),F^7,P^{34}]$ -NPY(**1a**)-siRNA complex.

3.3 | Cell viability

As off-target toxicity of siRNA is well known, it was of great interest to assess the peptide-siRNA complex for possible toxic side effect.³⁹ The resazurin-based cell viability assay provides a reliable method for evaluating the survival rate of treated cells. During this assay, cells are incubated with resazurin solution, which will be metabolized to resofurin in living cells and results in a detectable and quantifiable color change. Following a 24-h treatment with only the peptide led to minor decrease of about 10% of cell survival for peptides **1a**, **2a**, **3a**, and **5a**, whereas treatment with **4a** and **6a** had no toxic effects (Table 3). Treatment of the cells with the peptide-siRNA complex revealed no significant loss in cell viability. Notably, this outcome was consistent across all different peptide shuttles.

3.4 | Receptor activation

Modifications on peptide ligands can influence their ability to activate their native receptor as shown before.^{34,40} The peptides were modified with a peptide linker to enable siRNA binding and with TAMRA necessary for the assay set-up in imaging experiments. Testing of receptor activation was performed by an inositol monophosphate (IP1) accumulation assay. Here, co-transfection of chimeric $G\alpha_{qi}$ plasmid was used to activate phospholipase C in a G_q -dependent mechanism despite the Y_1R activates G proteins endogenously.⁴¹ Native IP1 is measured by HTRF in competition with fluorescently labeled IP1 as described in manufacturer's protocol. All peptides show high activity comparable to the wild type (Supporting Information). Complexation of siRNA and peptide resulted in slightly right shifted concentration-

response curves and thus slightly decreased EC_{50} values for the full-length $[F^7,P^{34}]$ -NPY variants, whereas siRNA complexation has no effect on receptor activation for the short NPY variants as shown in Table 3.

3.5 | Arrestin-3 recruitment

Arrestin-3 (arr-3) is known to mediate receptor internalization for many receptors including the Y_1R .⁴² A NanoBRET-based arr-3 recruitment assay was used to investigate this activity.³³ Transiently transfected HEK293 cells were stimulated for 5 min prior BRET measurement. $[K^4(K_8),F^7,P^{34}]$ -NPY (**1a**) and $[K^4(D-K_8),F^7,P^{34}]$ -NPY (**2a**) showed similar EC_{50} values compared to the native Y_1R ligand NPY (Figure 3A). The short NPY analogues showed strongly decreased EC_{50} values as well as E_{max} values as visualized in Figure 3B,C. Moreover, peptides **3a**, **4a**, **5a**, and **6a** showed precipitation issues for concentrations higher than 10^{-6} M and thus did not reach the plateau as depicted in Figure 3B,C. Values for EC_{50} and E_{max} are shown in Table 4. Comparing the peptide variants regarding their linker, almost similar arr-3 recruitment was found for L-lysine variants compared to the peptides with a D-lysine linker independent of the peptide backbone. However, $[K^{27}(Adm),P^{30},K^{31}(K_8),Bip^{32},L^{34}]$ -NPY(27-36) (**3a**) showed a 9-fold decrease and $[K^{27}(Lau),P^{30},K^{31}(K_8),Bip^{32},L^{34}]$ -NPY(27-36) (**5a**) a 14-fold decrease in EC_{50} value compared to $[K^4(K_8),F^7,P^{34}]$ -NPY (**1a**). For the D-lysine linker variants, the EC_{50} shift was ninefold for both short NPY variants in comparison to $[K^4(D-K_8),F^7,P^{34}]$ -NPY (**2a**).

3.6 | Internalization

Next, compounds were investigated for their internalization properties in order to deliver siRNA into specific cells by receptor-mediated uptake using a semiconfocal microscope equipped with an aptome. We were interested to find out whether peptides and siRNA co-internalize or whether the complex undergoes degradation during this process. For this purpose, Hepa1c1c7 cells were used, which express the Y_1R endogenously. Living cells were stimulated with either 1 μ M peptide (Figure 4), 1 μ M siRNA, or peptide-siRNA complex consisting of 1 μ M peptide and 200 nM siRNA for 60 min (Figure 5). Next, cells were subjected to thorough washing steps prior to microscopy imaging. In Figure 4, microscopy images of cells stimulated with 1 μ M peptide are shown. The microscopy analysis revealed distinct patterns across the various peptides tested. Peptides independent of their modification and backbone were able to internalize into cells expressing the Y_1R (Figure 4B) in a comparable manner, whereas stimulation of HEK293 cells without the Y_1R did not lead to any visible uptake (Figure 4A). However, administration of peptide-siRNA complex led to a more diverse result as shown in Figure 5. Notably, complex with siRNA and peptide **1** demonstrated co-internalization of the peptide and siRNA indicative of successful transport to intracellular compartments. In contrast, complex with siRNA and peptide **2** exhibited a noteworthy deviation, with the peptide dispersed throughout the cell

TABLE 3 Receptor activation of peptides determined by inositol phosphate accumulation assay at Y₁R in stably transfected COS-7 hY₁R ΔGq cells and percentage of surviving cells determined by resazurin-based cell viability assay. Ratio of peptide-siRNA complex was 5:1 (peptide/siRNA). N ≥ 3 independent experiments were conducted in triplicates. Statistical significance was tested with an ordinary one-way ANOVA, ***p < 0.001.

	Peptide	EC ₅₀ [nM]	pEC ₅₀	Surviving cells [%]
1a	[K ⁴ (K ₈),F ⁷ ,P ³⁴]-NPY	1.3	8.87 ± 0.08	89 ± 3 (**)
	[K ⁴ (K ₈),F ⁷ ,P ³⁴]-NPY + siRNA	4.2	8.38 ± 0.03	99 ± 1 (ns)
2a	[K ⁴ (D-K ₈),F ⁷ ,P ³⁴]-NPY	2.6	8.59 ± 0.05	90 ± 3 (**)
	[K ⁴ (D-K ₈),F ⁷ ,P ³⁴]-NPY + siRNA	2.5	8.60 ± 0.03	99 ± 1 (ns)
3a	[K ²⁷ (Adm),P ³⁰ ,K ³¹ (K ₈),Bip ³² ,L ³⁴]-NPY(27-36)	2.5	8.61 ± 0.03	89 ± 3 (*)
	[K ²⁷ (Adm),P ³⁰ ,K ³¹ (K ₈),Bip ³² ,L ³⁴]-NPY(27-36) + siRNA	3.0	8.52 ± 0.04	103 ± 3 (ns)
4a	[K ²⁷ (Adm),P ³⁰ ,K ³¹ (D-K ₈),Bip ³² ,L ³⁴]-NPY(27-36)	3.2	8.49 ± 0.03	101 ± 1 (ns)
	[K ²⁷ (Adm),P ³⁰ ,K ³¹ (D-K ₈),Bip ³² ,L ³⁴]-NPY(27-36) + siRNA	3.4	8.48 ± 0.04	102 ± 0 (ns)
5a	[K ²⁷ (Lau),P ³⁰ ,K ³¹ (K ₈),Bip ³² ,L ³⁴]-NPY(27-36)	2.3	8.64 ± 0.03	87 ± 3 (***)
	[K ²⁷ (Lau),P ³⁰ ,K ³¹ (K ₈),Bip ³² ,L ³⁴]-NPY(27-36) + siRNA	2.0	8.71 ± 0.02	102 ± 1 (ns)
6a	[K ²⁷ (Lau),P ³⁰ ,K ³¹ (D-K ₈),Bip ³² ,L ³⁴]-NPY(27-36)	2.5	8.60 ± 0.03	101 ± 0 (ns)
	[K ²⁷ (Lau),P ³⁰ ,K ³¹ (D-K ₈),Bip ³² ,L ³⁴]-NPY(27-36) + siRNA	2.2	8.65 ± 0.03	98 ± 1 (ns)
7	[F ⁷ ,P ³⁴]-NPY	0.7	9.18 ± 0.02	

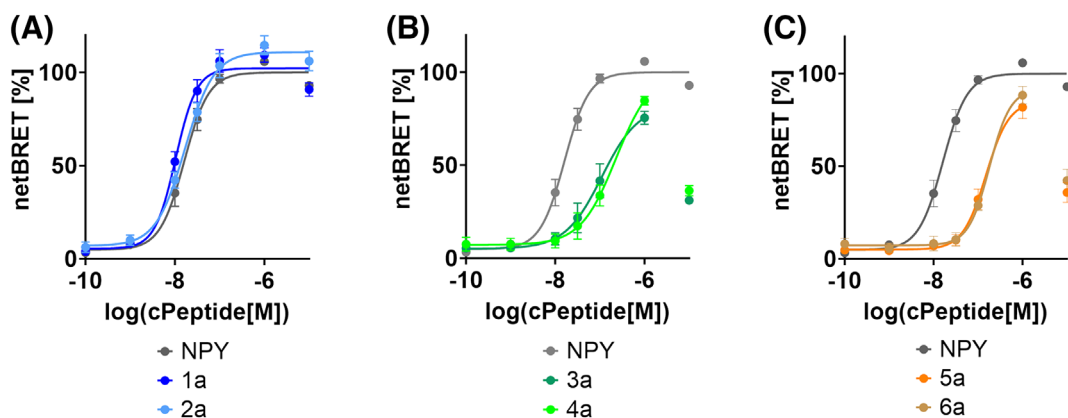


FIGURE 3 Arrrestin-3 (arr-3) recruitment BRET of NPY analogues. (A) Concentration-response curves of NPY and [K⁴(K₈),F⁷,P³⁴]-NPY analogues were measured 5 min after stimulation. [K⁴(D-K₈),F⁷,P³⁴]-NPY (2a) shows similar ability of arr-3 recruitment in comparison to [K⁴(K₈),F⁷,P³⁴]-NPY (1a). (B) Concentration-response curves of NPY and [K²⁷(Adm),P³⁰,K³¹(K₈),Bip³²,L³⁴]-NPY(27-36) (3a, 4a) analogues measured 5 min after stimulation. [K²⁷(Adm),P³⁰,K³¹(K₈),Bip³²,L³⁴]-NPY(27-36) (3a) shows similar ability of arr-3 recruitment compared to [K²⁷(Adm),P³⁰,K³¹(D-K₈),Bip³²,L³⁴]-NPY(27-36) (4a). (C) Concentration-response curves of NPY and [K²⁷(Lau),P³⁰,K³¹(K₈),Bip³²,L³⁴]-NPY(27-36) analogues (5a, 6a) were measured 5 min after stimulation. [K²⁷(Lau),P³⁰,K³¹(K₈),Bip³²,L³⁴]-NPY(27-36) (5a) shows a similar ability of arr-3 recruitment compared to [K²⁷(Lau),P³⁰,K³¹(D-K₈),Bip³²,L³⁴]-NPY(27-36) (6a).

TABLE 4 Arr-3 recruitment of peptides determined by NanoBRET-based arr-3 recruitment assay at Y₁R in transiently transfected HEK293 cells. N ≥ 3 independent experiments were performed in triplicates.

	Peptide	EC ₅₀ (pEC ₅₀ ± SEM)	E _{max}
1a	[K ⁴ (K ₈),F ⁷ ,P ³⁴]-NPY	10.4 (7.98 ± 0.06)	97
2a	[K ⁴ (D-K ₈),F ⁷ ,P ³⁴]-NPY	16.7 (7.78 ± 0.06)	104
3a	[K ²⁷ (Adm),P ³⁰ ,K ³¹ (K ₈),Bip ³² ,L ³⁴]-NPY(27-36)	≥94.5 (7.03 ± 0.11)	≥72
4a	[K ²⁷ (Adm),P ³⁰ ,K ³¹ (D-K ₈),Bip ³² ,L ³⁴]-NPY(27-36)	≥152.6 (6.82 ± 0.10)	≥78
5a	[K ²⁷ (Lau),P ³⁰ ,K ³¹ (K ₈),Bip ³² ,L ³⁴]-NPY(27-36)	≥138.9 (6.86 ± 0.08)	≥77
6a	[K ²⁷ (Lau),P ³⁰ ,K ³¹ (D-K ₈),Bip ³² ,L ³⁴]-NPY(27-36)	≥158.8 (6.80 ± 0.11)	≥81
	NPY	16.2 (7.79 ± 0.05)	95

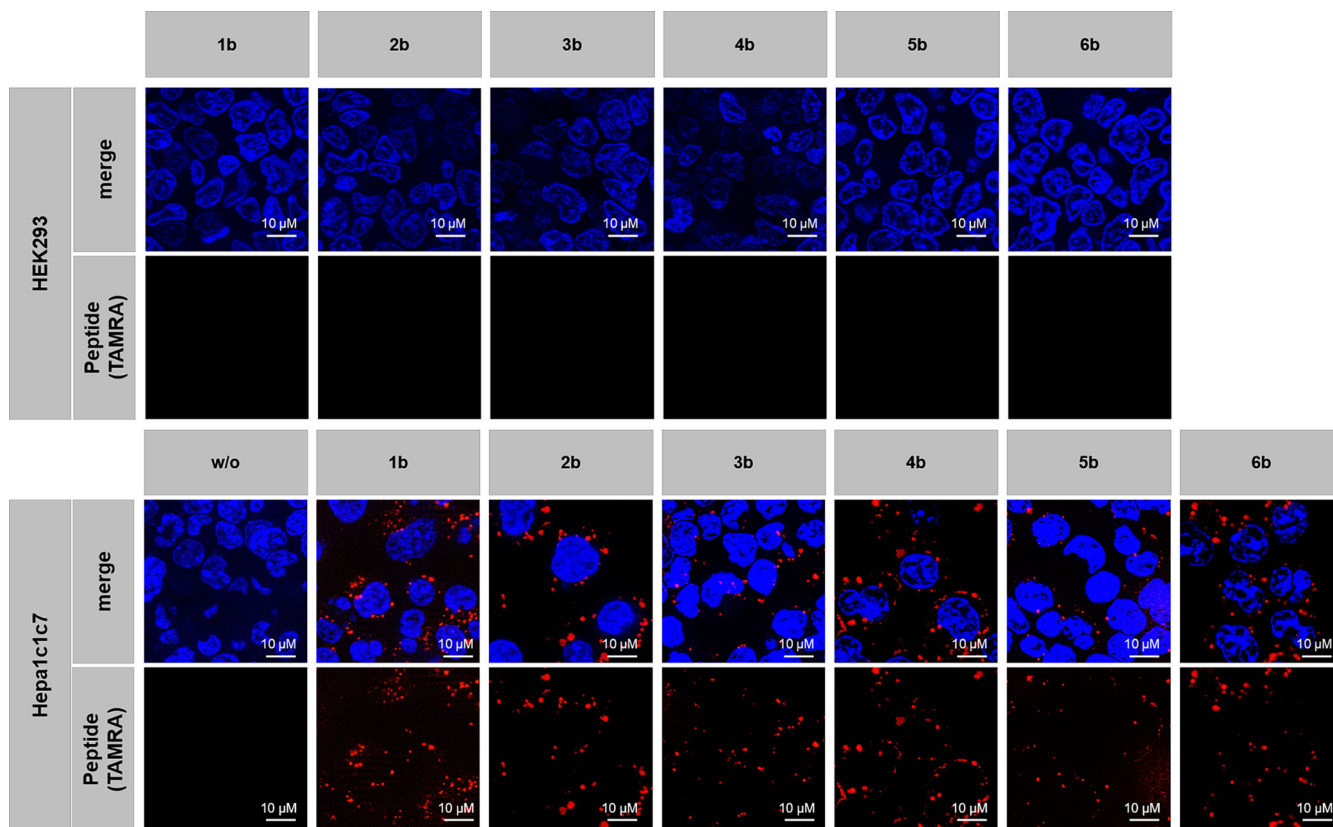


FIGURE 4 Characterization of Y_1R internalization. Live-cell image of HEK2993 (A) and Hepa1c1c7 cells (B). The cells were visualized by fluorescence microscopy prior to (w/o) and after stimulation with peptides 1–6. Cell nuclei were stained with Hoechst333342 dye (blue). Peptide fluorescence can be seen in red.

without apparent vesicles, suggesting precipitation of the complex on the cells. Complexes with siRNA and peptides 3, 4, 5, and 6 displayed successful co-internalization of peptide and siRNA comparable to complex 1, though displaying differences in siRNA detectability and vesicle size. In particular, peptide–siRNA complex with peptide 5 exhibited the presence of smaller vesicles compared to the other peptides. In conclusion, our microscopy experiments demonstrate effective internalization of the peptide–siRNA complexes for peptides 1 and 3–6, signifying their potential as delivery vehicles. However, the precipitation observed for peptide 2 requires further investigation to address its limitations as siRNA delivery platform.

3.7 | Gene knockdown

To assess whether the shuttled siRNA is able to reach the RISC complex and induce mRNA degradation, Hepa1c1c7 cells were incubated with peptide–siRNA complex consisting of 50 μ M of the corresponding peptide and 10 μ M siRNA for 6 h. After 72 h of growth time, cells were harvested, RNA was isolated, and quantitative real-time PCR was performed. As shown in Figure 6, the ability to achieve mRNA degradation differed significantly between the various complexes. To verify a receptor-mediated uptake of the peptide–siRNA complexes, cells were treated with an Y_1R antagonist BIBP3226 prior to stimulation with peptide–siRNA complex. Thus, specific effects if

peptide-mediated siRNA are indicated by the difference in gene expression.

Complexes with L-lysine linker variants (1a, 3a, 5a) achieved a decrease in mRNA expression to a range between 65% and 83%, independent of the different backbones. This suggests that L-lysine is rapidly degraded. Complexes with D-lysine linker variants show a broader range on the impact of a decreased mRNA expression varying between 39% and 88%. Here, a smaller peptide backbone is more efficient than the full-length peptide. Full-length peptide showed no specific uptake. This is in agreement with the precipitation shown in Figure 5.

For complexes with L-lysine linker variants (1a, 3a, 5a), treatment with BIBP3226 did not lead to a significant change in gene silencing efficiency. Full-length peptide with an D-lysine linker (2a) did not lead to a significant change in gene silencing efficiency as well, owing to the precipitation observed for this complex. For complexes of siRNA with 4a and 6a, the most significant gene silencing effect was found. This was partly (6a) or fully (4a) reverted by BIBP3226 treatment as shown in Figure 6. Especially for the complex with 4a, the mRNA degradation effect can be completely blocked by BIBP3226 treatment, whereas the effect of the complex with 6a has been decreased by at least 20% suggesting cell specific receptor-mediated uptake.

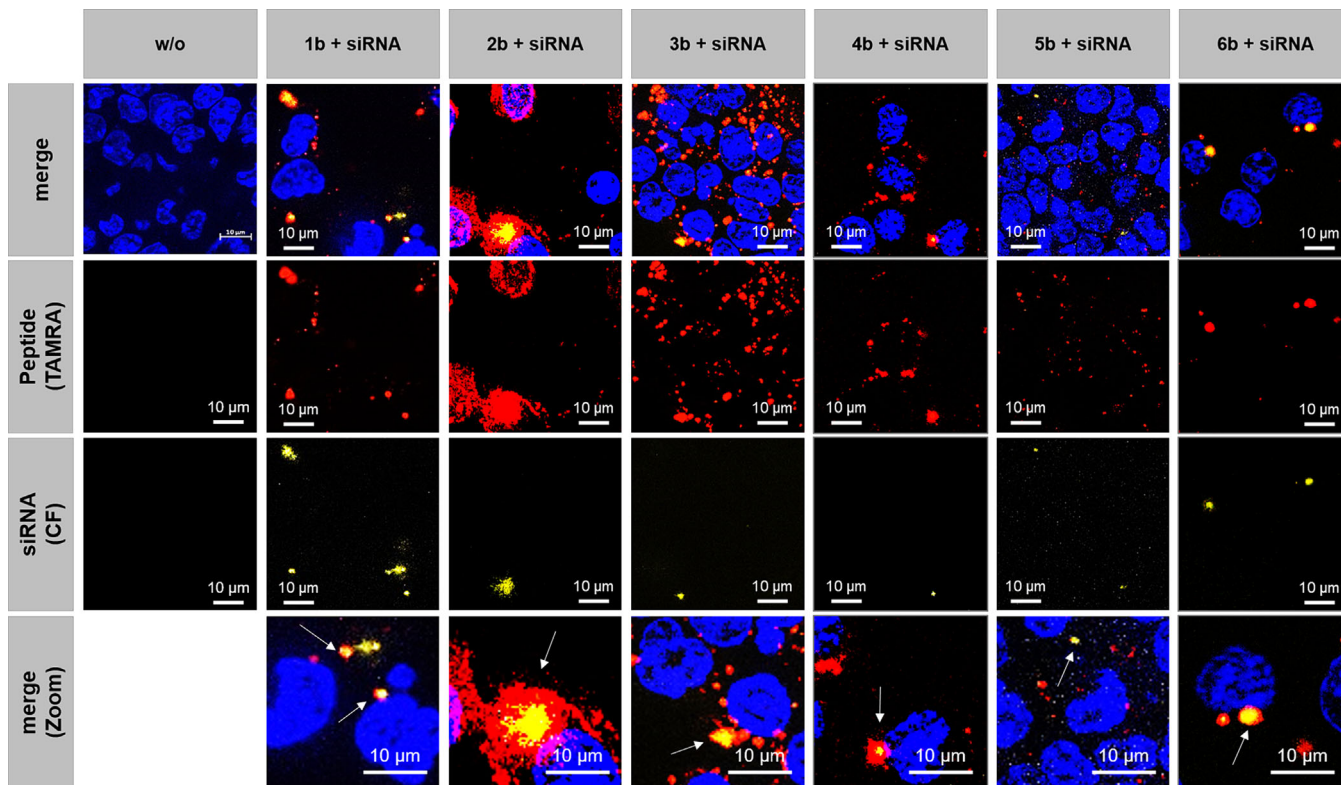
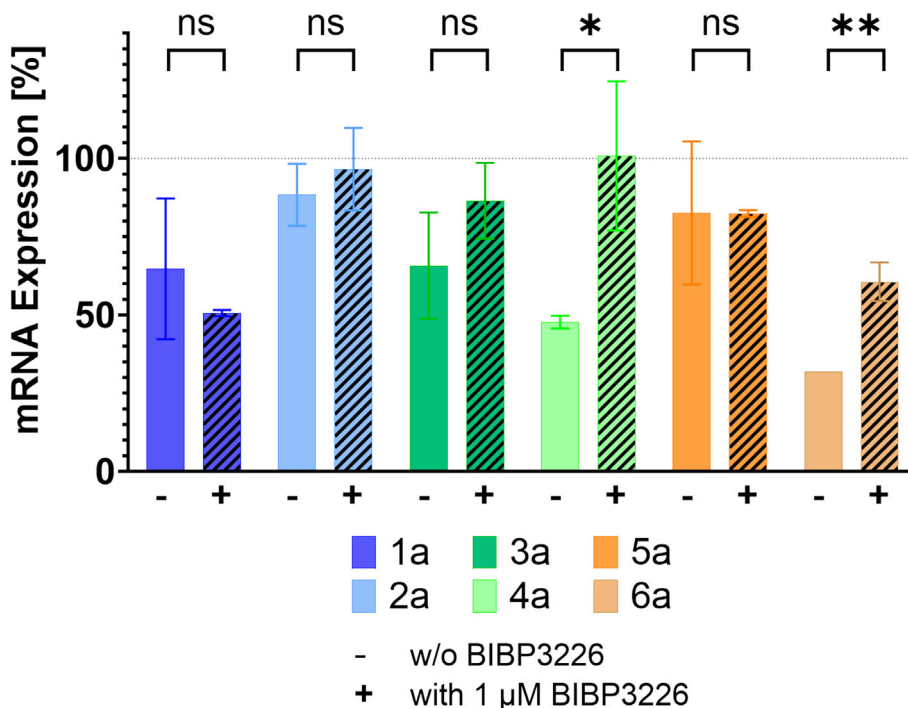


FIGURE 5 Characterization of Y₁R internalization. Live-cell image of Hepa1c1 cells. The cells were visualized by fluorescence microscopy prior to (w/o) and after stimulation with peptide–siRNA complex of different composition. Ratio of peptide–siRNA complex was 5:1 (peptide/siRNA). Cell nuclei were stained with Hoechst33342 dye (blue). Peptide fluorescence can be seen in red, and siRNA fluorescence is shown in yellow. Co-internalization of siRNA and peptide can be shown for all tested complex compositions.

FIGURE 6 qPCR and knockdown analysis of TSC22D4. qPCR quantitative expression analysis of TSC22D4 after administration of peptide–siRNA complex without (A) or with (B) the Y₁R antagonist BIBP3226. Ratio of peptide–siRNA complex was 5:1 (peptide/siRNA). Hepa1c1 cells were treated with the complex for 6 h, and cells were harvested approximately 72 h after incubation. Knockdown efficiency was examined by qPCR amplification of TSC22D4. The expression was normalized against Nono. Bars indicate the SEM of triplicate analyses. Statistical significance was tested with an unpaired, two-tailed t test.



4 | DISCUSSION

Effective siRNA delivery remains challenging in the field of targeted siRNA therapeutics.⁸ To address this, a multitude of strategies, including lipid-based delivery platforms and nanoparticles, have been explored.^{16,21} In our study, we apply peptide ligands as shuttle systems that had already been used in the delivery of toxins or transcription factor modulators.^{43,44} Our investigation focused on peptide analogues derived from the native Y₁R ligand NPY, each with distinct modifications in their attached linker and peptide backbone. This variation gave us the opportunity to question the influence of linker stability and size of the delivery platform on the performance of these peptide shuttle systems. Our comprehensive analysis covered evaluations of cell toxicity, Y₁R activation, arr-3 recruitment, internalization efficiency, and the influence of the delivery platform on gene silencing when complexed with siRNA. Understanding of the potential of peptide-based delivery systems was advanced, and valuable insights into optimizing the design for enhanced siRNA delivery were provided. Thus, our results contribute to the ongoing efforts aiming to overcome the challenges associated with RNA therapeutics.^{10–13}

As cell toxicity is a frequent issue throughout the different delivery platforms, peptides are an attractive option as they barely induce toxic side effects.²⁵ Even when modified with several hydrophilic residues or after complexation with siRNA no cytotoxicity has been observed.

It was already described that short NPY analogues show high receptor affinity but less efficient arr-3 recruitment and internalization. These characteristics were shown to be influenced by the peptide modification.²⁸ The short NPY analogues modified with a lauroyl moiety exhibit increased hydrophobicity, which was found to be important for signaling efficacy and potency as it increased abundance of the peptide at the membrane. However, arr-3 recruitment requires a bulky moiety more than hydrophobicity to fit into a binding pocket triggering arrestin recruitment.²⁸ All tested peptides displayed comparable EC₅₀ values in receptor activation in the range from 1.3 nM for [K⁴(K₈),F⁷,P³⁴]-NPY (**1a**) to 3.2 nM for [K²⁷(Adm),P³⁰,K³¹(D-K₈),Bip³²,L³⁴]-NPY(27-36) (**4a**). Interestingly, they did not tolerate complexation with siRNA in a comparable manner. For [K⁴(K₈),F⁷,P³⁴]-NPY (**1a**) receptor, activation ability decreased with a threefold shift, whereas for the adamantly-propionyl-modified short NPY (**3a**, **4a**), EC₅₀ values remained comparable shifting from 2.5 to 3.0 nM for **3a** and from 3.2 to 3.4 nM for **4a**. For the lauroyl variants (**5a**, **6a**), they even slightly improved from 2.3 to 2.0 nM for **5a** and from 2.5 to 2.2 nM for **6a**, respectively. For the short NPY analogues, linker composition did not influence their behavior after siRNA complexation. However, the full-length analogue tolerated complexation with siRNA slightly better when using D-K₈ linker. This confirms that performance of the peptide itself does not indicate the behavior of the peptide–siRNA complex.

The comparison of the performance of arr-3 recruitment shows that [K⁴(K₈),F⁷,P³⁴]-NPY (**1a**) has a 10–15 times advantage in potency as well as an improved efficacy over the short NPY analogues. In fact, it was already shown that short NPY analogues do not reach

comparable abilities as full-length ligands in arr-3 recruitment.²⁸ However, linker composition has only little influence on potency and efficacy in arr-3 recruitment.

Despite considerable differences in their ability to acquire arrestin upon receptor activation, all tested peptide constructs were able to induce internalization of the receptor. Peptide and siRNA were co-internalized hinting at an intact complex except for complexes with peptide **2a**. Since stimulation with siRNA alone did not result in cellular incorporation, receptor-mediated uptake of the peptide–siRNA complex is suggested. This is further supported by the experiments with cells that do not express the Y₁R and also display no uptake.

When evaluating the gene silencing efficiency of the various complexes, all tested complexes demonstrated a reduction in the corresponding mRNA expression, confirming the successful release of siRNA from endosomes and its delivery to the RISC as anticipated. In gene knockdown experiments, short NPY analogues exhibited superior efficiency compared to the full-length peptides, particularly when modified with a D-K₈ linker. Similar findings have been reported for arginine-based delivery platforms, where the inclusion of D-amino acids led to enhanced cellular uptake in comparison to platforms utilizing L-amino acids.⁴⁵ This demonstrates the favorable attributes of small but stable peptides as efficient shuttling systems. Furthermore, the tested short NPY variants possess nearly double the percentage of positive charges relative to their amino acid quantity compared to full-length peptides, which potentially enhances cell surface interaction, uptake, and shielding of siRNA from enzymatic degradation.⁴⁶ In contrast, in the case of larger peptide delivery platforms, a more labile linker variant proved advantageous, as complexes with [K⁴(K₈),F⁷,P³⁴]-NPY (**1**) exhibited greater effects on mRNA degradation compared to [K⁴(D-K₈),F⁷,P³⁴]-NPY (**2**), which was prone to precipitation after complexation with siRNA, thereby inhibiting internalization and access to the RNAi machinery. Additionally, application of the Y₁R antagonist BIBP3226 led to a reduction in gene silencing efficiency, providing further evidence of receptor-mediated uptake and specific cellular effects. This confirms the results of the internalization studies discussed above.

5 | CONCLUSION

In conclusion, our study shows that specific uptake of siRNA by GPCR-mediated internalization is possible and leads to cell-specific gene silencing. High-affinity peptides that activate this receptor can be equipped with an octalysine linker for siRNA complexation.

All complexes were able to activate the Y₁ receptor on a similar level, underwent cellular internalization, and downregulate mRNA expression. However, only D-K₈ linker at the short NPY ligands led to specific gene silencing that could be fully or partly inhibited with the antagonist BIBP3226. The complex using [K²⁷(Lau),P³⁰,K³¹(D-K₈),Bip³²,L³⁴]-NPY(27-36) (**6**) as delivery platform turned out to be superior and emphasizes the potential of this peptide as a robust and effective carrier for enhancing the efficacy of siRNA delivery strategies employing peptide shuttle systems.

ACKNOWLEDGEMENTS

The authors kindly acknowledge Ronny Müller and Kristin Löbner for their excellent technical support in matters of peptide synthesis and cell culture. Open Access funding enabled and organized by Projekt DEAL.

ORCID

Annette G. Beck-Sickinger  <https://orcid.org/0000-0003-4560-8020>

REFERENCES

1. Fire A, Xu S, Montgomery MK, Kostas SA, Driver SE, Mello CC. Potent and specific genetic interference by double-stranded RNA in *Caenorhabditis elegans*. *Nature*. 1998;391(6669):806-811. doi:10.1038/35888
2. Caplen NJ, Parrish S, Imani F, Fire A, Morgan RA. Specific inhibition of gene expression by small double-stranded RNAs in invertebrate and vertebrate systems. *PNAS*. 2001;98(17):9742-9747. doi:10.1073/pnas.171251798
3. Elbashir SM, Harborth J, Lendeckel W, Yalcin A, Weber K, Tuschl T. Duplexes of 21-nucleotide RNAs mediate RNA interference in cultured mammalian cells. *Nature*. 2001;411(6836):494-498. doi:10.1038/35078107
4. Charbe NB, Amnerkar ND, Ramesh B, et al. Small interfering RNA for cancer treatment: overcoming hurdles in delivery. *Acta Pharm Sin B*. 2020;10(11):2075-2109. doi:10.1016/j.apsb.2020.10.005
5. Jinek M, Doudna JA. A three-dimensional view of the molecular machinery of RNA interference. *Nature*. 2009;457(7228):405-412. doi:10.1038/nature07755
6. Leung RKM, Whittaker PA. RNA interference: from gene silencing to gene-specific therapeutics. *Pharmacol Ther*. 2005;107(2):222-239. doi:10.1016/j.pharmthera.2005.03.004
7. Ryther RCC, Flynt AS, Phillips JA, Patton JG. siRNA therapeutics: big potential from small RNAs. *Gene Ther*. 2005;12(1):5-11. doi:10.1038/sj.gt.3302356
8. Lu M, Xing H, Zheng A, Huang Y, Liang XJ. Overcoming pharmaceutical bottlenecks for nucleic acid drug development. *Acc Chem Res*. 2023;56(3):224-236. doi:10.1021/acs.accounts.2c00464
9. Hoy SM. Patisiran: first global approval. *Drugs*. 2018;78(15):1625-1631. doi:10.1007/s40265-018-0983-6
10. Whitehead KA, Langer R, Anderson DG. Knocking down barriers: advances in siRNA delivery. *Nat Rev Drug Discov*. 2009;8(2):129-138. doi:10.1038/nrd2742
11. Wang J, Lu Z, Wientjes MG, Au JL. Delivery of siRNA therapeutics: barriers and carriers. *AAPS J*. 2010;12(4):492-503. doi:10.1208/s12248-010-9210-4
12. Dominska M, Dykxhoorn DM. Breaking down the barriers: siRNA delivery and endosome escape. *J Cell Sci*. 2010;123(Pt 8):1183-1189. doi:10.1242/jcs.066399
13. Sajid MI, Moazzam M, Kato S, Cho KY, Tiwari RK. Overcoming barriers for siRNA therapeutics: from bench to bedside. *Pharmaceuticals*. 2020;13(10):294. doi:10.3390/ph13100294
14. Yuan X, Naguib S, Wu Z. Recent advances of siRNA delivery by nanoparticles. *Expert Opin Drug Deliv*. 2011;8(4):521-536. doi:10.1517/17425247.2011.559223
15. Gary DJ, Puri N, Won YY. Polymer-based siRNA delivery: perspectives on the fundamental and phenomenological distinctions from polymerbased DNA delivery. *J Control Release*. 2007;121(1-2):64-73. doi:10.1016/j.jconrel.2007.05.021
16. Lin Q, Chen J, Zhang Z, Zheng G. Lipid-based nanoparticles in the systemic delivery of siRNA. *Nanomedicine*. 2014;9(1):105-120. doi:10.2217/nnm.13.192
17. Zhou J, Patel TR, Fu M, Bertram JP, Saltzman WM. Octa-functional PLGA nanoparticles for targeted and efficient siRNA delivery to tumors. *Biomaterials*. 2012;33(2):583-591. doi:10.1016/j.biomaterials.2011.09.061
18. Loh XJ, Lee TC, Dou Q, Deen GR. Utilising inorganic nanocarriers for gene delivery. *Biomater Sci*. 2016;4(1):70-86. doi:10.1039/C5BM00277J
19. Stuart DD, Kao GY, Allen TM. A novel, long-circulating, and functional liposomal formulation of antisense oligodeoxynucleotides targeted against MDR1. *Cancer Gene Ther*. 2000;7(3):466-475. doi:10.1038/sj.cgt.7700145
20. Hafez IM, Maurer N, Cullis PR. On the mechanism whereby cationic lipids promote intracellular delivery of polynucleic acids. *Gene Ther*. 2001;8(15):1188-1196. doi:10.1038/sj.gt.3301506
21. Guo S, Li K, Hu B, et al. Membrane-destabilizing ionizable lipid empowered imaging-guided siRNA delivery and cancer treatment. *Exp Dermatol*. 2021;1(1):35-49. doi:10.1002/EXP.20210008
22. Lu S, Morris VB, Labhasetwar V. Effectiveness of small interfering RNA delivery via arginine-rich polyethylenimine-based polyplex in metastatic and doxorubicin-resistant breast cancer cells. *J Pharmacol Exp Ther*. 2019;370(3):902-910. doi:10.1124/jpet.119.256909
23. Luong D, Kesharwani P, Deshmukh R, et al. PEGylated PAMAM dendrimers: enhancing efficacy and mitigating toxicity for effective anti-cancer drug and gene delivery. *Acta Biomater*. 2016;43:14-29. doi:10.1016/j.actbio.2016.07.015
24. Sakurai Y, Hatakeyama H, Sato Y, et al. Endosomal escape and the knockdown efficiency of liposomal-siRNA by the fusogenic peptide shGALA. *Biomaterials*. 2011;32(24):5733-5742. doi:10.1016/j.biomaterials.2011.04.047
25. Ahrens VM, Bellmann-Sickert K, Beck-Sickinger AG. Peptides and peptide conjugates: therapeutics on the upward path. *Future Med Chem*. 2012;4(12):1567-1586. doi:10.4155/fmc.12.76
26. Mäde V, Els-Heindl S, Beck-Sickinger AG. Automated solid-phase peptide synthesis to obtain therapeutic peptides. *Beilstein J Org Chem*. 2014;10:1197-1212. doi:10.3762/bjoc.10.118
27. Söll RM, Dinger MC, Lundell I, Larhammer D, Beck-Sickinger AG. Novel analogues of neuropeptide Y with a preference for the Y₁-receptor. *Eur J Biochem*. 2001;268(10):2828-2837. doi:10.1046/j.1432-1327.2001.02161.x
28. Hofmann S, Lindner J, Beck-Sickinger AG, Hey Hawkins E, Bellmann-Sickert K. Carbaboranylation of truncated C-terminal neuropeptide Y analogue leads to full hY₁ receptor agonism. *ChemBioChem*. 2018;19(21):2300-2306. doi:10.1002/cbic.201800343
29. Demir S, Wolff G, Wieder A, et al. TSC22D4 interacts with Akt1 to regulate glucose metabolism. *Sci Adv*. 2022;8(42):eabo5555. doi:10.1126/sciadv.abo5555
30. Ekim Üstünel B, Friedrich K, Maida A, et al. Control of diabetic hyperglycaemia and insulin resistance through TSC22D4. *Nat Commun*. 2016;7(1):13267. doi:10.1038/ncomms13267
31. Goto N, Suzuki H, Zheng L, et al. Promotion of squamous cell carcinoma tumorigenesis by oncogene-mediated THG-1/TSC22D4 phosphorylation. *Cancer Sci*. 2023;114(10):3972-3983. doi:10.1111/cas.15934
32. Wanka L, Babilon L, Kaiser A, Mörl K, Beck-Sickinger AG. Different mode of arrestin-3 binding at the human Y₁ and Y₂ receptor. *Cell Signal*. 2018;50:58-71. doi:10.1016/j.cellsig.2018.06.010
33. Hall MP, Unch J, Binkowski BF, et al. Engineered luciferase reporter from a deep sea shrimp utilizing a novel imidazopyrazinone substrate. *ACS Chem Biol*. 2012;7(11):1848-1857. doi:10.1021/cb3002478
34. Mäde V, Bellmann-Sickert K, Kaiser A, Meiler J, Beck-Sickinger AG. Position and length of fatty acids strongly affect receptor selectivity pattern of human pancreatic polypeptide analogues. *ChemMedChem*. 2014;9(11):2463-2474. doi:10.1002/cmdc.201402235

35. Unnamalai N, Kang BG, Lee WS. Cationic oligopeptide-mediated delivery of dsRNA for post-transcriptional gene silencing in plant cells. *FEBS Lett.* 2004;566(1):307-310. doi:[10.1016/j.febslet.2004.04.018](https://doi.org/10.1016/j.febslet.2004.04.018)
36. Won YW, Yoon SM, Lee KM, Kim YH. Poly (oligo-D-arginine) with internal disulfide linkages as a cytoplasm-sensitive carrier for siRNA delivery. *Mol Ther.* 2011;19(2):372-380. doi:[10.1038/mt.2010.242](https://doi.org/10.1038/mt.2010.242)
37. Zhang C, Tang N, Liu XJ, Liang W, Xu W, Torchilin VP. siRNA-containing liposomes modified with polyarginine effectively silence the targeted gene. *J Control Release.* 2006;112(2):229-239. doi:[10.1016/j.jconrel.2006.01.022](https://doi.org/10.1016/j.jconrel.2006.01.022)
38. Wang YH, Hou YW, Lee HJ. An intracellular delivery method for siRNA by an arginine-rich peptide. *J Biochem Biophys Methods.* 2007;70(4):579-586. doi:[10.1016/j.jbbm.2007.01.010](https://doi.org/10.1016/j.jbbm.2007.01.010)
39. Hu B, Zhong L, Weng Y, et al. Therapeutic siRNA: state of the art. *Sig Transduct Target Ther.* 2020;5(1):101. doi:[10.1038/s41392-020-0207-x](https://doi.org/10.1038/s41392-020-0207-x)
40. Mäde V, Babilon S, Jolly N, et al. Peptide modifications differentially alter G protein-coupled receptor internalization and signaling bias. *Angew Chem Int Ed.* 2014;53(38):10067-10071. doi:[10.1002/anie.201403750](https://doi.org/10.1002/anie.201403750)
41. Kostenis E. Is Gα16 the optimal tool for fishing ligands of orphan G-protein-coupled receptors? *Trends Pharmacol Sci.* 2001;22(11):560-564. doi:[10.1016/s0165-6147\(00\)01810-1](https://doi.org/10.1016/s0165-6147(00)01810-1)
42. Gurevich VV, Gurevich EV. GPCRs and signal transducers: interaction stoichiometry. *Trends Pharmacol Sci.* 2018;39(7):672-684. doi:[10.1016/j.tips.2018.04.002](https://doi.org/10.1016/j.tips.2018.04.002)
43. Böhme D, Beck-Sickinger AG. Drug delivery and release systems for targeted tumor therapy. *J Pept Sci.* 2015;21(3):186-200. doi:[10.1002/psc.2753](https://doi.org/10.1002/psc.2753)
44. Wittrisch S, Klötting N, Mörl K, Chakaroun R, Blüher M, Beck-Sickinger AG. NPY₁R-targeted peptide-mediated delivery of a dual PPARα/γ agonist to adipocytes enhances adipogenesis and prevents diabetes progression. *Mol Metab.* 2020;31:163-180. doi:[10.1016/j.molmet.2019.11.009](https://doi.org/10.1016/j.molmet.2019.11.009)
45. Wender PA, Mitchell DJ, Pattabiraman K, Pelkey ET, Steinman L, Rothbard JB. The design, synthesis, and evaluation of molecules that enable or enhance cellular uptake: peptoid molecular transporters. *PNAS.* 2000;97(24):13003-13008. doi:[10.1073/pnas.97.24.13003](https://doi.org/10.1073/pnas.97.24.13003)
46. Samec T, Alatisé KL, Boulos J, et al. Fusogenic peptide delivery of bioactive siRNAs targeting CSNK2A1 for treatment of ovarian cancer. *Mol Ther Nucleic Acids.* 2022;30:95-111. doi:[10.1016/j.omtn.2022.09.012](https://doi.org/10.1016/j.omtn.2022.09.012)

SUPPORTING INFORMATION

Additional supporting information can be found online in the Supporting Information section at the end of this article.

How to cite this article: Schenk M, Mörl K, Herzig S, Beck-Sickinger AG. Targeted modulation of gene expression through receptor-specific delivery of small interfering RNA peptide conjugates. *J Pept Sci.* 2024;e3611. doi:[10.1002/psc.3611](https://doi.org/10.1002/psc.3611)